Microbial Biotechnology

WILEY

MICROBIAL BIOTECHNOLOGY Open Access

RESEARCH ARTICLE OPEN ACCESS

Evolutionary Trajectories of Methionine Metabolism in *Mycobacterium* and Its Application to Engineer a Vitamin B12 Whole-Cell Ribosensor

Elena Campos-Pardos[1,2] | Laura Sanz-Asensio[1] | Sandra Pérez-Jiménez[1] | Inmaculada Yruela[3,4] | Bruno Contreras-Moreira[3,4] | Alejandro Toledo-Arana[5] | Jesús Gonzalo-Asensio[1,2]

[1]Grupo de Genética de Micobacterias, Departamento de Microbiología, Facultad de Medicina, Universidad de Zaragoza, IIS Aragón, Zaragoza, Spain | [2]CIBER Enfermedades Respiratorias, Instituto de Salud Carlos III, Madrid, Spain | [3]Estación Experimental de Aula Dei (EEAD), CSIC, Zaragoza, Spain | [4]Grupo de Bioquímica, Biofísica y Biología Computacional (BIFI, UNIZAR), Unidad Asociada I+D+i al CSIC, Zaragoza, Spain | [5]Instituto de Agrobiotecnología (IDAB). CSIC-Gobierno de Navarra, Mutilva, Spain

Correspondence: Jesús Gonzalo-Asensio (jagonzal@unizar.es)

Received: 20 November 2024 | **Revised:** 21 May 2025 | **Accepted:** 25 May 2025

Funding: This work was supported by Gobierno de Aragón, DGA predoctoral contract to LSA. Ministerio de Ciencia, Innovación y Universidades, FPU17/02909, PID2019-104690RB-I00, PID2023-148710OB-I00.

Keywords: B12 metabolism | cobalamin | methionine biosynthesis | *Mycobacterium tuberculosis* complex | non-tuberculous mycobacteria

ABSTRACT

Vitamin B12 metabolism differs among members of the *Mycobacterium* genus. While non-tuberculous mycobacterial species are B12 producers, tuberculous mycobacteria lack endogenous production and rely on the host supply of this vitamin. Here, we hypothesise that this discrepant phenotype might impact the function of B12-dependent enzymes. We specifically focused on methionine synthases MetH and MetE. Both enzymes showed genetic differences in the *Mycobacterium* genus, resulting in a clear divergence between tuberculous and non-tuberculous species. Unexpectedly, the dependency of MetH on B12 was indistinguishable between *M. tuberculosis* and *M. smegmatis*, assayed as representative members of tuberculous and non-tuberculous species, respectively. However, MetE showed robust phenotypic differences between these species, displaying a finely tuned B12 regulation in *M. tuberculosis*, in contrast to a more permissive regulation in *M. smegmatis*. Both orthologs differ in the vitamin isoform specifically recognised, and the B12 threshold level required for MetE regulation. Since the B12 regulatory element in the *metE* gene is an RNA riboswitch, we analysed the polymorphisms in this region, with a special focus on loss-of-function mutations identified after in vitro selection. We used this information to engineer a whole-cell B12 biosensor in the genetically fastidious *Mycobacterium* genus, being able to detect vitamin B12 concentration in the range of micrograms per millilitre.

1 | Introduction

Vitamin B12 (B12) or cobalamin (Cbl) is the most structurally complex of all vitamins and biological cofactors, and it is required in diverse metabolic pathways in both prokaryotes and animals (Hodgkin et al. 1955). Cbl refers to a group of molecules constituted by a cobinamide precursor, consisting of a cobalt-containing corrinoid ring, coordinated with a variable group that determines the different isoforms of this vitamin (Warren et al. 2002). Despite being an essential nutrient for many organisms, its *de novo* biosynthesis is limited to certain archaea and bacteria, with no evidence of eukaryotic synthesis (Roth

Elena Campos-Pardos and Laura Sanz-Asensio contributed equally to this article.

et al. 1996). Therefore, animals, including humans, must obtain Cbl through the diet.

As mentioned, B12 plays a critical role in both animal and bacterial metabolism. Animals possess two B12-dependent enzymes: R-methylmalonyl-CoA mutase and methionine synthase, involved in methylmalonate metabolism and methionine biosynthesis, respectively (Young et al. 2015). These enzymes can also be found in bacteria and archaea, which additionally harbour other B12-dependent enzymes. In fact, three classes of B12-dependent enzymes have been recognised in the bacterial world: isomerases, methyltransferases, and reducing dehalogenases (Shelton et al. 2019). In addition to its role as enzyme cofactor, B12 also influences bacterial metabolism by regulating gene expression through riboswitches. Riboswitches are evolutionary conserved non-coding RNA regions, typically embedded within the 5′ UTR of bacterial mRNAs, able to bind specific metabolites and modulate gene expression (Nahvi et al. 2004). B12 riboswitches are widely distributed in 5′ UTR B12-related genes in eubacteria, and are commonly found upstream of genes for B12 biosynthesis, B12 transport or B12-dependent metabolic pathways (Vitreschak et al. 2003).

Tuberculosis (TB) is an airborne infectious disease caused by microorganisms of the *Mycobacterium tuberculosis* Complex (MTBC), which caused 1.25 million deaths in 2023 (World Health Organization 2024). The MTBC is comprised by a highly clonal group of TB-causing ecotypes that are adapted to different animal hosts, being *M. tuberculosis* and *M. africanum* the ones adapted to humans. *M. cannetti*, an occasional human pathogen, is considered to be the progenitor and common ancestor of the MTBC (Broset et al. 2015). The genus *Mycobacterium* also includes non-tuberculous mycobacteria (NTM), which are ubiquitous in nature, and generally opportunistic (such as *M. avium* or *M. abscessus*) or non-pathogenic (such as *M. smegmatis*) (Riojas et al. 2018).

B12 is thought to influence mycobacterial metabolism through the two mechanisms aforementioned. On the one hand, it is a cofactor for three B12-dependent enzymes in *M. tuberculosis* (Gopinath et al. 2013). One of these three enzymes is the methionine synthase MetH, which is responsible for converting homocysteine to L-methionine (Met) using B12 as a cofactor (Figure 1A). Specifically, it catalyses the transfer of the methyl group from the methyl-tetrahydrofolate to homocysteine, forming Met (Pejchal and Ludwig 2005). On the other hand, B12

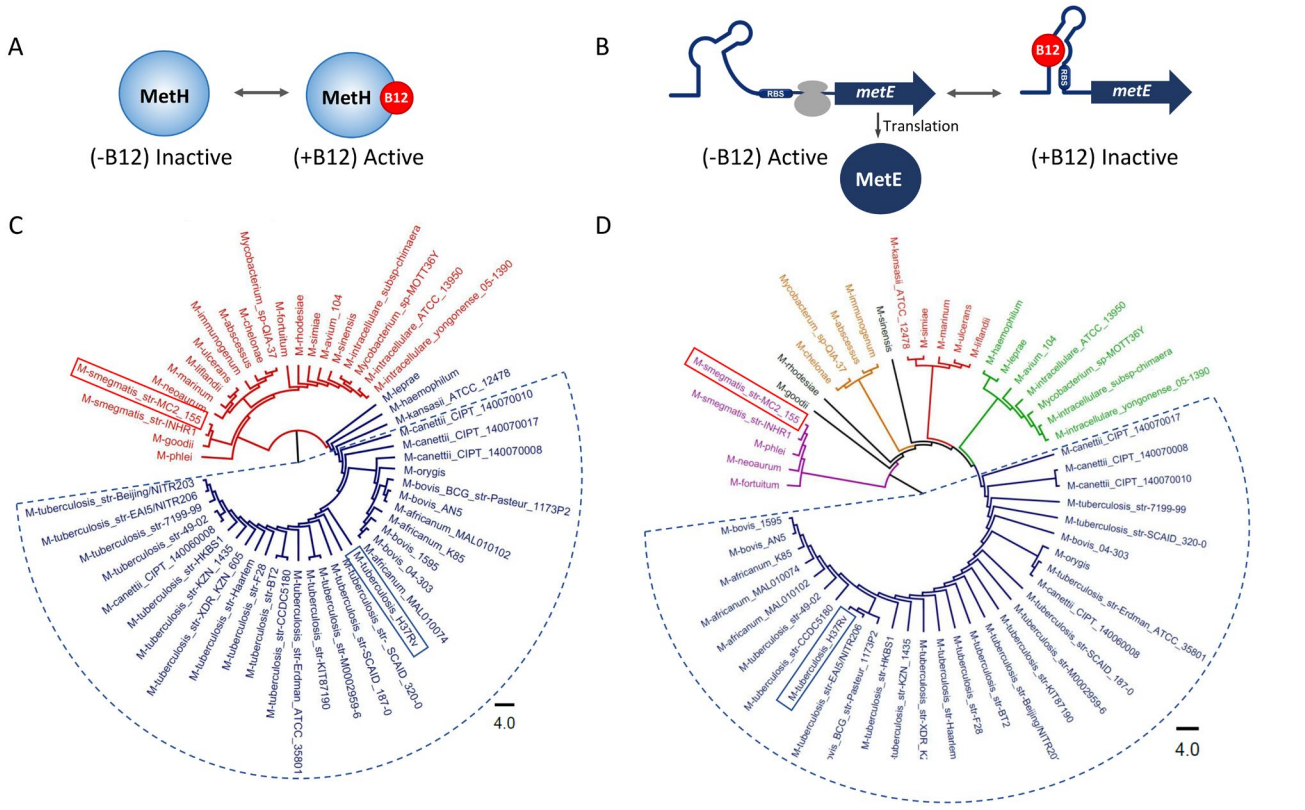

FIGURE 1 | B12-dependent regulation of the methionine synthases MetH and MetE and their phylogenetic relationships in *Mycobacterium*. (A) Schematic representation of MetH activity illustrating its dependence on B12 as cofactor for enzymatic function. (B) Schematic representation of B12-dependent regulation of MetE. Expression of MetE is regulated by a riboswitch located upstream of the *metE* mRNA. When B12 is absent, the *metE* gene is expressed and MetE is produced. However, when B12 binds to the riboswitch, it causes conformational changes in this RNA region which avoid proper expression of *metE*. (C and D) Phylogenetic trees showing the evolutionary relationships of MetH (C) and MetE (D) among 153 *Mycobacterium* sequences, covering the MTBC (114 sequences) and NTM (39 sequences). The MTBC clade is indicated by a dotted line. *M. tuberculosis* H37Rv and *M. smegmatis* mc^{2}155, used in this study as representative species of the MTBC and NTM, are highlighted in blue and red boxes, respectively.

regulates gene expression by binding to two riboswitch-regulated operons in the *M. tuberculosis* transcriptome, in both cases preventing protein production (Warner et al. 2007; Campos-Pardos et al. 2024; Kipkorir et al. 2024). One operon comprises *PPE2*, *cobQ1* and *cobU* genes (Vitreschak et al. 2003), while the other one encodes the methionine synthase MetE. This enzyme also catalyses the final step of Met biosynthesis, by the same reaction as MetH, but does not use B12 as a cofactor (Warner et al. 2007; Gopinath et al. 2013) (Figure 1B). Therefore, Met biosynthesis in *M. tuberculosis* is catalysed by two complementary methionine synthases: MetE, whose synthesis is repressed by a B12 riboswitch located upstream of the *metE* gene, or MetH, which requires B12 as a cofactor (Figure 1).

In a previous work, we evidenced the crucial role of B12 in host-TB interactions (Campos-Pardos et al. 2024). We observed that the MTBC has evolved through a genomic decay for B12 biosynthesis, while *M. cannetti* and environmental mycobacteria are still able to produce endogenous B12. However, all these species possess B12-dependent enzymes and retain the capacity for B12 exogenous uptake. Accordingly, we demonstrated that MTBC bacteria scavenge B12 from the host to modulate their virulence. The B12 transcriptome of the MTBC corroborated methionine biosynthesis as a key B12-regulated phenotype, elucidating a plausible connection among TB virulence, B12 uptake, and methionine metabolism.

Considering these previous findings, here we have focused our study on the Met metabolism from an evolutionary perspective. Here, we highlight two main differential factors in the regulation of *M. smegmatis* and *M. tuberculosis metE* B12-riboswitches: the B12 isoform that acts as a natural ligand, and the minimum concentration of the specific isoform required to activate the repression mechanisms. Finally, we apply this knowledge to engineer a B12 ribosensor in mycobacteria.

2 | Results

2.1 | MetE and MetH Exhibit Phylogenetic Differences Between Tuberculous and Non-Tuberculous Mycobacteria

The genetic differences in B12 biosynthesis previously determined, along with the role of B12 in the regulation of Met metabolism (Campos-Pardos et al. 2024), prompted us to determine whether MetE and MetH had differentially evolved between the MTBC and NTM species. To achieve this goal, we calculated MetE and MetH phylogenetic trees, querying the amino acid sequences of these proteins in several representative mycobacterial species (Figure 1, Table S1). In both phylogenies, all strains from the MTBC positioned in the same branch of the tree (bootstrap > 96), indicating a high conservation of MetH (Figure 1C) and MetE (Figure 1D) enzymes in these strains, which correlates with the fact that the MTBC is composed of a highly clonal group of TB-causing ecotypes (Broset et al. 2015). However, MetH and MetE from opportunistic, non-pathogenic, and environmental mycobacteria are positioned in other clades (bootstrap > 96), and phylogenetically separated from the MTBC (Figure 1C,D). MetH and MetE from *M. canettii* strains, considered as the MTBC most recent ancestor, lie between the MTBC and NTM species (bootstrap > 99), supporting the evolutionary hypothesis that the MTBC evolved from an environmental bacterium that eventually infected a mammalian host and specialised to survive intracellularly (Jang et al. 2008).

To continue studying the interaction between B12 and Met metabolism from an evolutionary perspective, we selected three representative mycobacterial species: *M. tuberculosis* H37Rv, which belongs to the MTBC and is routinely used as a reference strain since its initial sequencing in 1998 (Cole et al. 1998); *M. smegmatis* mc^{2}155, which is considered an environmental, fast-growing NTM and is used as a non-pathogenic laboratory model for genetic experiments (Snapper et al. 1990); and *M. canettii* C59, selected as a representative ancestor of the MTBC to bridge the gap between this group and NTM (Supply et al. 2013).

2.2 | MetH Orthologs Exhibit Comparable B12 Dependency Between the MTBC and NTM Despite Their Phylogenetic Differences

In mycobacteria, the final step of Met synthesis is complementarily synthesised by MetE and MetH enzymes. Thus, to specifically study the role of each Met synthase, it is necessary to delete its complementary isoenzyme. We first focused on the B12-dependent MetH isoform (Figure 1A) by studying *metE* gene deletion mutants in *M. tuberculosis* H37Rv, *M. smegmatis* mc^{2}155 and *M. canetti* C59 (Figure S1). We and others have previously demonstrated that NTM are B12 producers (Minias et al. 2021; Campos-Pardos et al. 2024). Accordingly, to rule out the effect of endogenous B12 in *M. smegmatis*, we first abrogated B12 production in this species by a genomic deletion of *cobLMK* genes (Figure 2A). This B12 mutant was constructed in a two-step process: first, we replaced the *cobLMK* genes with a kanamycin resistance marker; then, we unmarked the mutation with the objective of recycling the antibiotic cassette for the downstream deletion of *metE* (Figure 2B). Finally, we validated the absence of B12 production in the final, unmarked, Δ*cobLMK* strain (Figure 2C).

We evaluated the in vitro phenotype of the aforementioned Δ*metE* mutants in the absence or presence of different B12 isoforms. Specifically, we used adenosylcobalamin (AdoCbl), methylcobalamin (MeCbl) and hydroxylcobalamin (OHCbl), which are physiological isoforms of B12, and cyanocobalamin (CNCbl), which is a synthetic isoform. As expected, we confirmed a total lack of in vitro growth in solid media of H37Rv Δ*metE* and mc^{2}155 Δ*cobLMK* Δ*metE* in the absence of B12 (Figure 3). Interestingly, when we supplemented the medium with MeCbl, the specific isoform that acts as MetH cofactor (Jarrett et al. 1996; Goulding et al. 1997), in vitro growth of both mutants was restored. Besides, the mutants were capable of growing in the presence of the other B12 isoforms, whether they were physiological or synthetic (Figure 3). *M. canettii* C59 Δ*metE* showed the same in vitro dependency on B12 as H37Rv Δ*metE* (Figure S2). However, we observed that *M. canettii* C59 Δ*metE* grew slightly better without B12 than H37Rv Δ*metE*. This result suggests that endogenous production of B12 by *M. canettii* C59 might be sufficient to support a residual MetH functionality, but the intrinsic B12 levels fail to guarantee optimal growth. On the one hand, these results demonstrate the

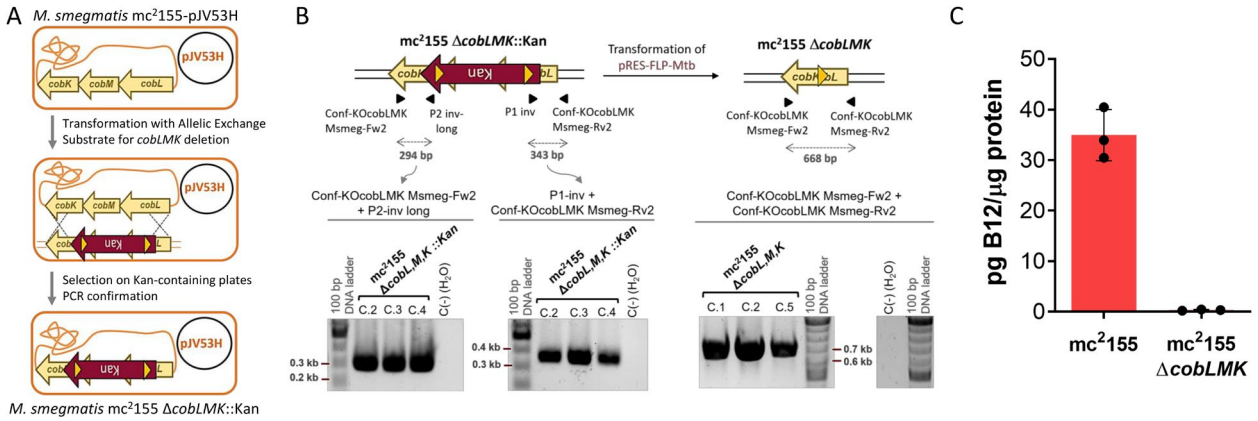

FIGURE 2 | Generation and validation of a Δ*cobLMK* mutant in *Mycobacterium smegmatis* mc²155. (A) Schematic representation of the genetic steps for the KO construction of the *cobLMK* operon in *M. smegmatis* mc²155. The allelic exchange substrate (AES) targeting the *cobLMK* region was amplified from the pKD4 plasmid, and includes a kanamycin (Kan) resistance cassette. This AES was transformed in the mc²155 strain carrying the recombineering machinery in the pJV53H plasmid. After recombineering, the AES replace the *cobLMK* operon and allows selection of the Δ*cobLMK*::Kan mutant on Kan plates. (B) Confirmation of the recombination event involving the insertion of the Kan resistance cassette in the *cobLMK* locus. PCR verification was performed using specific primers that bind upstream and downstream of the recombination site and within the resistance cassette. In a next step, the Kan resistance cassette was resolved using the FRT sites (yellow triangles) and a resolvase-bearing plasmid (pRES-FLP-Mtb). Resolution of the resistance marker was confirmed by visualisation of the appropriate PCR band using primers located in the *cobL* and *cobK* genes. (C) Validation of abrogated B12 production in the *M. smegmatis* mc²155 Δ*cobLMK* mutant lacking the Kan resistance cassette. B12 levels were quantified in bacterial extracts from cultures of wild-type and Δ*cobLMK* mutant strains, confirming the absence of B12 biosynthesis in the mutant. Data from three independent experiments are shown as individual data points. Bars represent the mean and error bands indicate the standard deviation (SD).

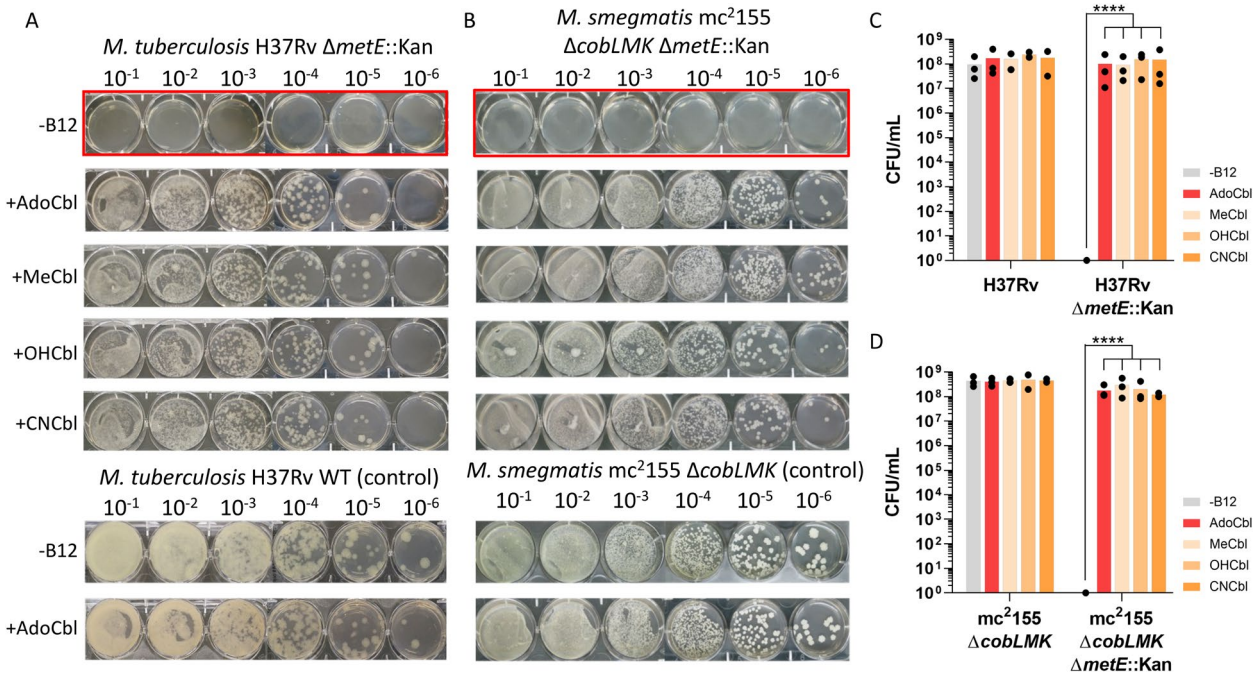

FIGURE 3 | Growth phenotypes of *M. tuberculosis* and *M. smegmatis metE* mutants in response to different B12 isoforms. This figure illustrates the dependency of MetH activity on cobalamin (Cbl) isoforms for optimal bacterial growth. (A) Serial dilutions of *M. tuberculosis* H37Rv Δ*metE*::Kan mutant and wild-type (WT) strain (used as control) were grown on media supplemented with different Cbl isoforms at 10 µg/mL: No B12 (-B12), adenosylcobalamin (+AdoCbl), methylcobalamin (+MeCbl), hydroxocobalamin (+OHCbl), and cyanocobalamin (+CNCbl). (B) Serial dilutions of *M. smegmatis* mc²155 Δ*cobLMK* Δ*metE*::Kan mutant and the Δ*cobLMK* single mutant (used as control) were grown under the same Cbl supplementation conditions depicted in panel A. In panels A and B, those bacterial dilutions showing markedly reduced growth compared to controls are highlighted with red boxes. (C) Bar graph showing colony-forming units per millilitre (CFU/mL) for *M. tuberculosis* H37Rv WT and Δ*metE*::Kan mutant, grown under the conditions described in panel A. A significant growth reduction was observed in the absence of Cbl supplementation. (D) Bar graph showing CFU/mL for *M. smegmatis* mc²155 Δ*cobLMK* Δ*metE*::Kan mutant and the Δ*cobLMK* single mutant under the same conditions. A significant growth reduction was also observed without Cbl supplementation. The *Y*-axis in panels C and D is displayed on a base-10 logarithmic scale. Data from three independent experiments are shown as individual data points. Only statistically significant differences ($p < 0.05$) are indicated.

existence of efficient B12 transport mechanisms in *M. tuberculosis* and *M. smegmatis*, as well as their capacity to metabolise different B12 isoforms into MeCbl, required as MetH cofactor. Finally, these results reconfirm the lack of *de novo* B12 synthesis in *M. tuberculosis* (Minias et al. 2021; Campos-Pardos et al. 2024). Altogether, MetH isoforms from *M. tuberculosis*, *M. canettii*, and *M. smegmatis* Δ*metE* mutants exhibited a clear dependence on B12, regardless of their evolutionary divergence within the *Mycobacterium* genus.

2.3 | MetE Orthologs Are Differentially Regulated by B12 in Tuberculous and Non-Tuberculous Mycobacteria

Next, we studied the in vitro phenotype of Δ*metH* mutants in *M. tuberculosis* H37Rv, *M. canettii* C59 and *M. smegmatis* mc^{2}155 (Figure S3). This latter mutant was constructed in the mc^{2}155 Δ*cobLMK* background to rule out the regulatory effect of B12 intrinsically produced by *M. smegmatis*. Since these mutants lack MetH, they are only capable of synthesising L-Met by the B12-independent MetE isoform. Consequently, they are all expected to show a deficient growth in the presence of B12, due to the repression exerted by this vitamin through the *metE* B12-riboswitch (Figure 1B).

The aforementioned Δ*metH* mutants were grown in solid medium in the absence or presence of the different B12 isoforms. H37Rv Δ*metH* properly grew in the absence of B12, while a significant growth reduction was observed under AdoCbl supplementation (Figure 4). This observation is consistent with previous studies that reported AdoCbl as the ligand that directly binds to the *metE* B12-riboswitch with high affinity and specificity, leading to the repression of the *metE* gene (Vitreschak et al. 2003; Nahvi et al. 2004). However, some H37Rv Δ*metH* colonies were still able to grow under AdoCbl pressure. This is probably due to the emergence of spontaneous mutants, which could have accumulated suppressor mutations affecting the *metE* B12-riboswitch function as previously documented (Warner et al. 2007; Campos-Pardos et al. 2024). This hypothesis will be further tested below, after interrogation of the *metE* riboswitch sequences from H37Rv Δ*metH* mutant colonies grown in the presence of AdoCbl. Nevertheless, we acknowledge that other unrelated polymorphisms-i.e. those affecting B12 transport identified by others (Gopinath et al. 2013)-, might be contributing to the emergence of *M. tuberculosis* Δ*metH* resistant colonies to the external B12 pressure. On the other hand, some H37Rv Δ*metH* colonies were able to grow in the presence of the other three B12 isoforms, although they showed a reduced growth, measured by colony size, compared to standard conditions (Figure 4). This

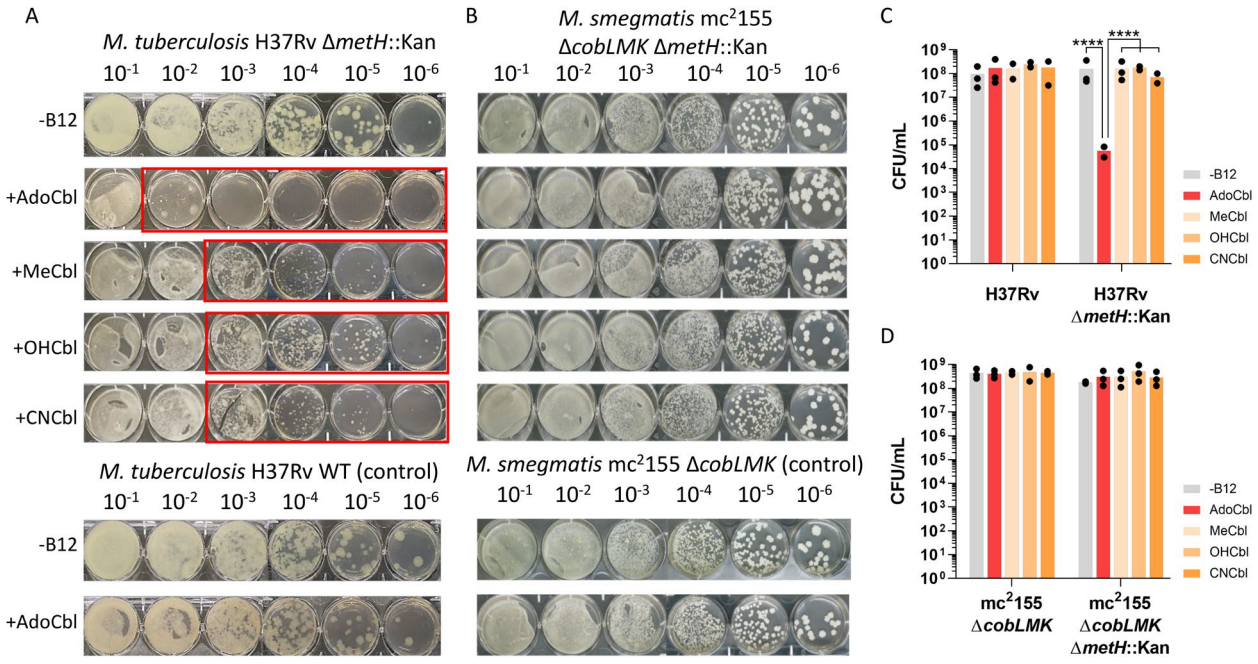

FIGURE 4 | Growth phenotypes of *M. tuberculosis* and *M. smegmatis metH* mutants in response to different B12 isoforms. This figure shows the dependency of the *M. tuberculosis* MetE ortolog on adenosylcobalamin, and to a lesser extent on other Cbl isoforms. This dependency is not observed in *M. smegmatis*. (A) Evaluation of bacterial growth of *M. tuberculosis* H37Rv Δ*metH*::Kan mutant and WT strain (used as control) on media supplemented with different Cbl isoforms at 10 μg/mL: No B12 (−B12), adenosylcobalamin (+AdoCbl), methylcobalamin (+MeCbl), hydroxocobalamin (+OHCbl), and cyanocobalamin (+CNCbl). (B) Growth of *M. smegmatis* mc^{2}155 Δ*cobLMK* Δ*metH*::Kan mutant compared to the Δ*cobLMK* single mutant (used as control) under the same Cbl supplementation conditions described in panel A. In panels A and B, red boxes highlight bacterial dilutions with reduced growth compared to their respective controls. (C) Bar graph showing CFU/mL for *M. tuberculosis* H37Rv WT and Δ*metH*::Kan mutant, grown under the conditions described in panel A. A significant growth reduction was observed under AdoCbl supplementation. (D) Bar graph showing CFU/mL for *M. smegmatis* mc^{2}155 Δ*cobLMK* Δ*metH*::Kan mutant and the Δ*cobLMK* single mutant under the same conditions. No growth reduction was observed with any Cbl isoform. The *Y*-axis in panels C and D is displayed on a base-10 logarithmic scale. Data from three independent experiments are shown as individual data points. Only statistically significant differences ($p < 0.05$) are indicated.

finding suggests that MeCbl, OHCbl or CNCbl isoforms could non-specifically bind to the *metE* B12-riboswitch, leading to reduced MetE expression. Another possibility might be the delayed conversion of these B12 isoforms into AdoCbl in *M. tuberculosis*. *M. canettii* C59 Δ*metH* mutant showed the same in vitro phenotype as H37Rv Δ*metH* (Figure S4). We also observed that *M. canettii* C59 Δ*metH* showed reduced growth in the presence of a B12 pressure compared to H37Rv Δ*metH* (Figure 4). This result might indicate that endogenous production of B12 by *M. canettii* C59 somehow contributes to the repression of the *metE* B12-riboswitch. In the case of *M. smegmatis* mc^{2}155 Δ*cobLMK* Δ*metH*, we observed equivalent growth compared to the Δ*cobLMK* control in the absence of B12 (Figure 4). Surprisingly, in contrast to H37Rv Δ*metH* or C59 Δ*metH*, neither AdoCbl supplementation nor the other three isoforms of this vitamin suppressed *M. smegmatis* growth. This result indicates that the *metE* B12-riboswitch is possibly less responsive in *M. smegmatis* compared to tuberculous mycobacteria.

2.4 | The *metE* Riboswitch in *M. smegmatis* Requires a Higher Concentration Threshold and Responds to Different B12 Isoforms Compared to Tuberculous Mycobacteria

Regulation by riboswitches occurs when the regulatory metabolite exceeds a concentration threshold. Therefore, we hypothesize that B12 supplementation at the single concentration used in our experiments on solid media might not be sufficient to repress the *metE* B12-riboswitch in *M. smegmatis* (Figure 4).

These intriguing results prompted us to analyse the response threshold of the *metE* riboswitch and its specificity for B12 isoforms in both *M. smegmatis* and *M. tuberculosis*. We grew H37Rv Δ*metH* and mc^{2}155 Δ*cobLMK* Δ*metH* in the presence of various concentrations of AdoCbl, MeCbl and CNCbl. Since H37Rv Δ*metH* already shows growth inhibition at 10 μg/mL, we used a concentration range from 0.001 to 100 μg/mL. In the case of mc^{2}155 Δ*cobLMK* Δ*metH*, since 10 μg/mL had not affected its growth in solid medium, we used a concentration range from 10 to 200 μg/mL (Figure 5). Consistent with our previous findings, AdoCbl-which is the specific ligand of the *metE* riboswitch- significantly inhibited H37Rv Δ*metH* growth even at the lowest concentration tested (0.001 μg/mL), while supplementation with MeCbl or CNCbl allowed bacterial growth up to a concentration of 10 μg/mL. At the maximum concentration of 100 μg/mL, all the isoforms completely inhibited the growth of H37Rv Δ*metH* (Figure 5A). Collectively, these results confirm AdoCbl as the preferred ligand for the *metE* riboswitch in *M. tuberculosis* and suggest a non-specific binding of MeCbl and CNCbl to this riboswitch, albeit at higher concentrations compared to AdoCbl. The mc^{2}155 Δ*cobLMK* Δ*metH* mutant grew when supplemented with 10 μg/mL of the three B12 isoforms. However, when raising the concentration to 20 μg/mL, both AdoCbl and MeCbl significantly suppressed bacterial growth, while the CNCbl artificial isoform required four-fold more concentration to elicit a comparable reduction in bacterial growth (Figure 5B). As occurred with the Δ*metH* mutants of *M. tuberculosis*, the residual colonies that grew at inhibitory concentrations may correspond to suppressor mutants of the *metE* riboswitch function. These results suggest that the *metE* riboswitch in *M. smegmatis* is less sensitive and has a broader range of B12 ligands compared to its ortholog in *M. tuberculosis*.

On the other hand, we studied the in vitro phenotype of the mc^{2}155 Δ*cobLMK* Δ*metH* mutant in liquid medium, in which metabolites are theoretically more accessible for their uptake compared with solid media. We evaluated bacterial growth in the absence or presence of different B12 isoforms at concentrations ranging from 0.001 to 100 μg/mL. The *metE* riboswitch in *M. smegmatis* showed a concentration-dependent activation, since bacterial growth gradually decreased with increasing concentrations of B12 (Figure 5C). This result might indeed indicate higher B12 bioavailability in liquid vs solid media. However, a significant arrest in bacterial growth was only observed when AdoCbl and MeCbl concentrations reached a concentration of 10 μg/mL, consistent with our findings on solid media. Corroborating our findings on solid media, a complete inhibition of bacterial growth occurred at a concentration of 100 μg/mL of the three B12 isoforms (Figure 5C). To validate these results, we evaluated bacterial viability after a 48 h treatment with B12 isoforms at the aforementioned concentrations. Following this incubation period, bacteria were plated on solid media, or used to perform a MTT-based assay to enumerate metabolically active bacteria. Results corroborated that incubation with more than 10 μg/mL of B12 isoforms resulted in bacterial killing (Figure S5).

Altogether, when comparing the phenotypic behaviour of *M. smegmatis* mc^{2}155 and *M. tuberculosis* H37Rv *metE* riboswitches, two main differential factors can be highlighted: the B12 isoform that could act as a natural ligand of the riboswitch, and the minimum concentration of this isoform required to repress the expression of *metE*. The *M. tuberculosis* riboswitch is able to sense concentrations as low as 0.001 μg/mL AdoCbl, while the corresponding regulatory element in *M. smegmatis* mc^{2}155 is responsive to around 2000-fold higher concentrations of both AdoCbl and MeCbl.

2.5 | The *metE* Riboswitch of *M. tuberculosis* and *M. smegmatis* are Polymorphic Sequences

Since the B12 response element responsible for *metE* regulation is located in the riboswitch, we first explored whether this sequence has differentially evolved during mycobacterial evolution. We performed a BLASTN search in the NCBI nt database to identify similar sequences to the *metE* riboswitch of *M. tuberculosis* H37Rv in other mycobacteria. Notably, all species from the MTBC showed a 100% identity. The ancestor *M. canettii* differs in a unique nucleotide and shows 99.53% identity. NTM showed greater genetic divergence and, particularly *M. smegmatis*, showed a 65% identity related to *M. tuberculosis* (Figure 6A,C). These observations also correlate with the phylogenetic analysis of MetE protein sequences from NTM, which split into five subgroups (Figure 1D).

The RNA secondary structure of the *M. tuberculosis metE* riboswitch has been studied recently (Kipkorir et al. 2024), and it is divided into two regions: an aptamer responsible for the B12-binding, and a regulatory region which controls expression

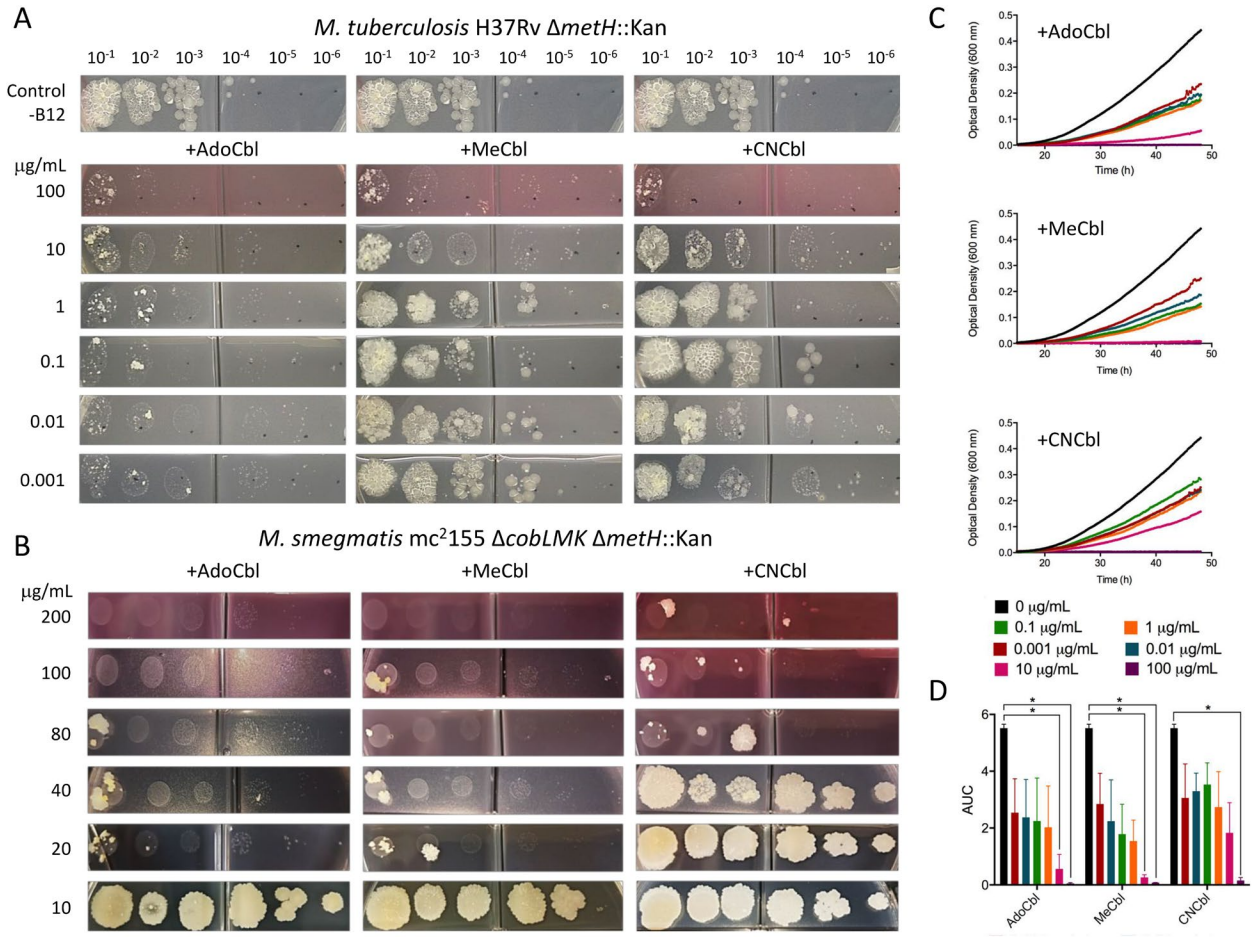

FIGURE 5 | Dose-dependent bacterial growth of MetE from *M. tuberculosis* and *M. smegmatis*. (A and B) Growth of *M. tuberculosis* H37Rv Δ*metH*::Kan (A) and *M. smegmatis* mc²155 Δ*cobLMK* Δ*metH*::Kan (B) on media supplemented with adenosylcobalamin (AdoCbl), methylcobalamin (MeCbl), and cyanocobalamin (CNCbl) at concentrations ranging from 0.001 to 200 µg/mL. Cultures without B12 supplementation and supplemented with 10 µg/mL AdoCbl were used as growth controls for *M. tuberculosis* and *M. smegmatis* respectively. (C) Growth curves of the *M. smegmatis* mc²155 Δ*cobLMK* Δ*metH*::Kan mutant under varying concentrations of cobalamin isoforms, demonstrating a concentration-dependent inhibition of growth. (D) Bar graph showing the area under the curve (AUC) of values shown in panel C, enumerating the overall growth response at different concentrations of B12 isoforms. Significant growth reduction was observed at 10 µg/mL and higher concentrations, with adenosylcobalamin (AdoCbl) and methylcobalamin (MeCbl) showing stronger inhibitory effects compared to cyanocobalamin (CNCbl). Error bars represent the standard error of the mean (SEM) from three independent experiments. Only statistically significant differences ($p < 0.05$) are indicated.

of the *metE* downstream gene (Figure 6B). Depending on the presence of B12, this RNA structure can shift between two conformations. When B12 is present, binding of this molecule to the aptamer favours the formation of a stem loop between the translation initiation region (TIR) and the αTIR region. As a consequence, the Shine-Dalgarno sequence located in the TIR segment is occluded, avoiding expression of *metE*. This structure is stabilised by formation of a kissing loop between the aptamer and a stem loop formed by the ααTIR segment (Figure 6B). When B12 is absent, a conformational change in the aptamer disrupts the formation of the kissing loop. This otherwise favours the formation of a stem loop between the ααTIR and αTIR segments, freeing the TIR region. In this conformation, the Shine-Dalgarno sequence is accessible for *metE* expression (Figure 6B).

We used this information to interrogate the differences in the *metE* riboswitches from *M. tuberculosis* and *M. smegmatis*. Despite the modest identity between both molecules, we found that the aptamer region is more conserved (68.9% identity) than the regulatory region (54.9%). Notably, those regions spanning the kissing loop, which include part of the B12-responsive element and the ααTIR stem loop, show the highest level of conservation (Figure 6C). On the other hand, to confirm the hypothesis that mutations in the riboswitch may abrogate B12 sensing, we decided to interrogate the riboswitch region from the *M. tuberculosis metH* mutant colonies grown in the presence of B12 pressure (Figure 4). After successful regrowth of 68 colonies on agar plates supplemented with AdoCbl, we sequenced the riboswitch region and identified 18 mutations in 16 positions of the *M. tuberculosis* riboswitch putatively abrogating B12 sensing. Further confirming the importance of these polymorphisms, it is interesting to note that some mutations were observed in multiple colonies. Confirming the essential role of these nucleotides in this B12 responsive element, we found that 15 of the 16 mutated positions are located in conserved regions between the *M. tuberculosis* and *M. smegmatis* riboswitches (Figure 6C). Mapping of these mutations to the riboswitch structure suggested that B12 binding could be compromised (Figure 6D), but additional work is

needed to interrogate the precise role of each polymorphism over B12 sensing by the riboswitch. Taken together, the conservation between *metE* riboswitches in *Mycobacterium* supports the B12 regulatory role in this genus, but genetic differences might explain the discrepancies in B12 sensing and *metE* regulation across species.

2.6 | Construction of a B12 Ribosensor Using the *metE* Riboswitch From *M. tuberculosis*

The *metE* riboswitch of *M. tuberculosis* has demonstrated improved sensitivity and selectivity compared to its *M. smegmatis* ortholog. This led us to use this element to construct a riboswitch-based biosensor (ribosensor) to detect B12. We identified the B12 riboswitch transcript after examination of previous RNA-seq data (Solans et al. 2014) (Figure 7A). We also studied the putative *metE* promoter to determine the consensus TANNNT sequence found in 73% of promoter sequences located upstream of transcription starting sites (TSSs) in *M. tuberculosis* (Cortes et al. 2013) (Figure 7A). We used this information to place the *metE* riboswitch and promoter sequences upstream of the *gfp* gene optimised for its expression in *Mycobacterium* (*eGFP*) (Figure 7B). This construction was cloned in a mycobacterial integrative plasmid, and the correct integration into the *M. tuberculosis* H37Rv chromosome was confirmed by PCR (Figure S6).

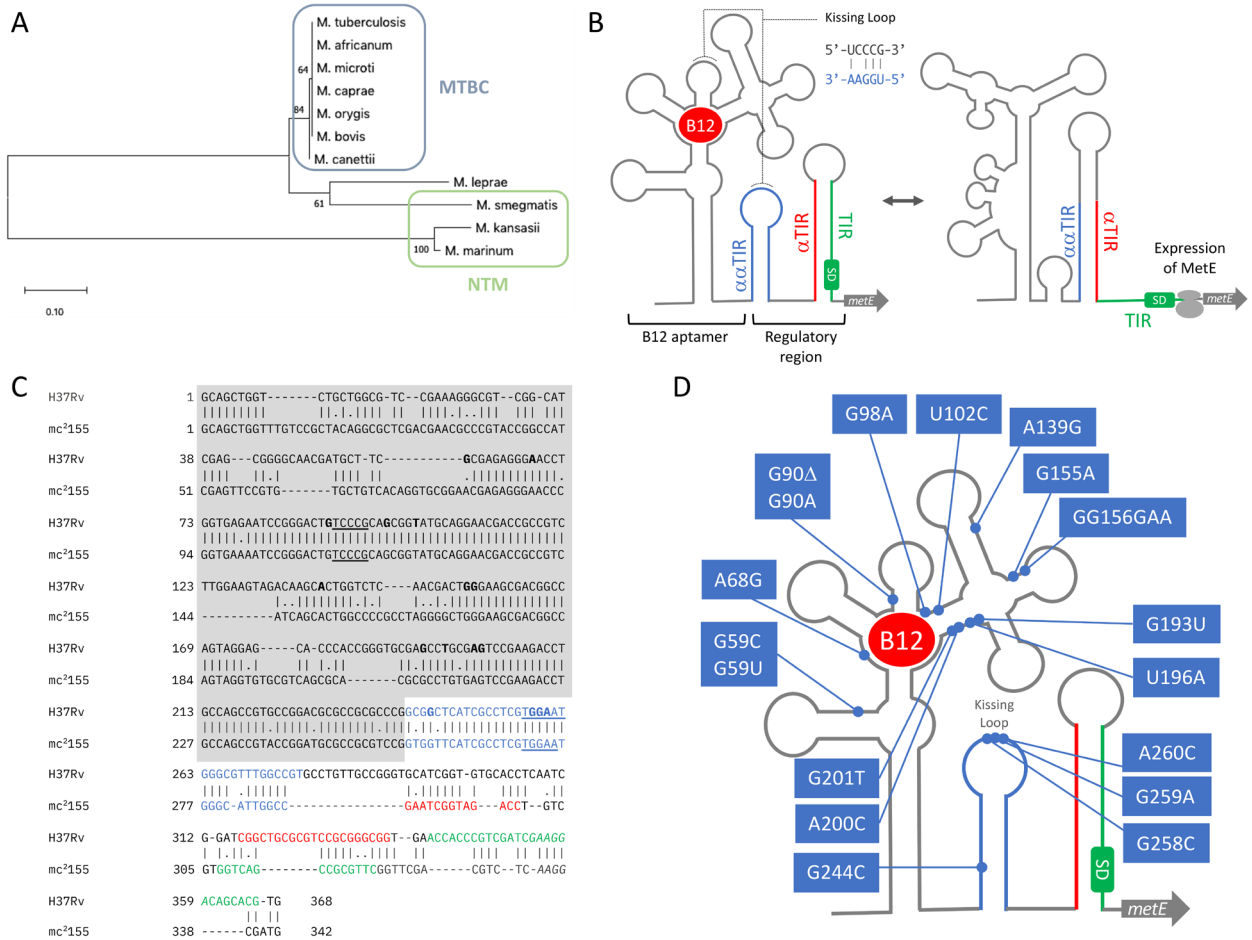

FIGURE 6 | Comparative analysis of the *metE* riboswitch in *Mycobacterium* species. (A) Phylogenetic tree of *metE* riboswitch sequences across different *Mycobacterium* species, with members of the MTBC and NTM highlighted in blue and green boxes, respectively. Bootstrap values are shown at each node. The tree was constructed using the Maximum Likelihood method with MEGA X. (B) Proposed mechanism of action of the *metE* riboswitch, according to previous studies (Vitreschak et al. 2003; Kipkorir et al. 2024). The figure shows secondary structures of the 5′ end of *metE* mRNA when B12 is present (left side) or absent (right side). The riboswitch consists on a B12 binding module named the aptamer (grey) and a regulatory region which consists on complementary terminator-antiterminator structures. When B12 binds to the aptamer, its favours the formation of a stem loop between the Translation Initiation Region (TIR) (green) and its αTIR (red). This structure is favoured by a kissing loop between the B12 aptamer and a loop in the ααTIR (blue). Formation of this structure occludes the Shine-Dalgarno (SD) sequence halting translation of the *metE* gene by the ribosome. In the absence of B12, the aptamer alters its conformation and favours the formation of a stem loop between the ααTIR and αTIR segments. In this conformation, the TIR region is accessible to the ribosome for translation of the *metE* gene. (C) Pairwise sequence alignment of *M. tuberculosis* H37Rv and *M. smegmatis* mc²155 *metE* riboswitches. The B12 aptamer is shaded in grey. The ααTIR, αTIR and TIR segments are coloured in blue, red and green, respectively. Sequences of the kissing loop are underlined. Putative SD sequences are in italics. Previously identified B12 escape mutations in *M. tuberculosis* are shown in bold characters. (D) Mapping of B12 suppressor mutations (shown in bold in panel C) in the secondary structure of the *metE* riboswitch. Note that these mutations affect to either the B12 binding motif, or to the formation of the kissing loop.

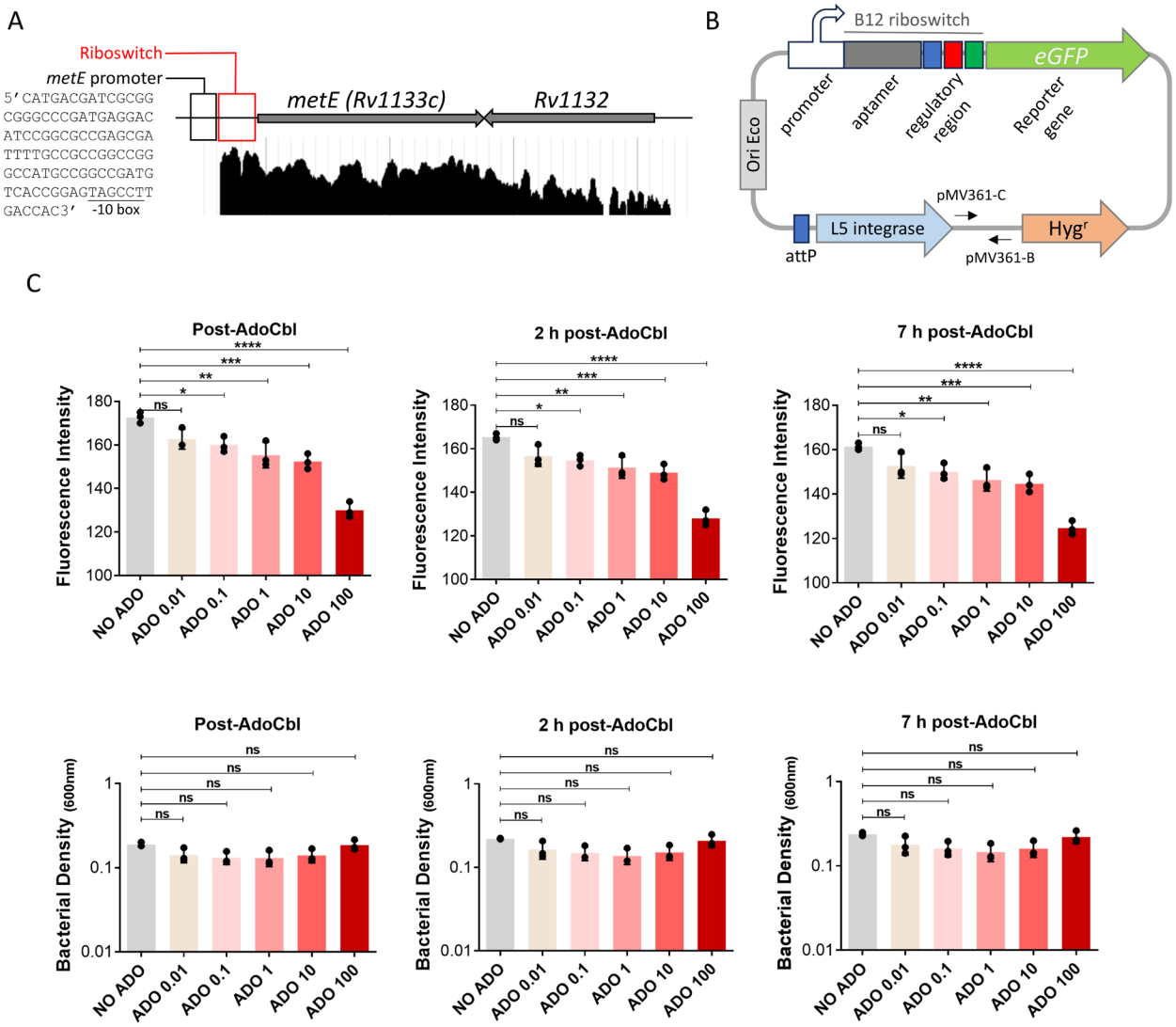

FIGURE 7 | Construction of a whole-cell B12 ribosensor in *Mycobacterium*. (A) RNA-seq profile of *metE* mRNA. Note the 5′ untranslated region corresponding to the riboswitch. The location of the predicted promoter is also indicated. (B) Construction of the B12 ribosensor by placing the B12 riboswitch from *M. tuberculosis* upstream of the GFP reporter gene. This construction was cloned in a mycobacterial integrative plasmid. Each genetic part is indicated in the diagram. The location of primers used to confirm the proper integration of the plasmid into the *M. tuberculosis* chromosome is also indicated. (C) Validation of the whole-cell B12 ribosensor. Upper panels show the fluorescence intensity emitted by the B12-ribosensor strain after the addition of increasing concentrations of AdoCbl. Different panels correspond to measurements immediately after the addition of AdoCbl, or after 2 and 7 h of incubation with AdoCbl. Lower panels show the reciprocal bacterial density (OD_{600}) values of cultures used in the upper panels.

The functionality of the ribosensor was validated upon incubation of the *M. tuberculosis* biosensor strain with different concentrations of AdoCbl. We observed a dose-dependent effect of B12 over GFP fluorescence, observing a gradual decrease in fluorescence with higher concentrations of the vitamin (Figure 7C). Albeit the ribosensor was able to detect AdoCbl concentrations as low as 0.01 μg/mL, we found that statistical significance was reached at 0.1 μg/mL. Notably, detection of AdoCbl was immediate, since fluorescence reading after addition of B12 produced an instant significant decrease in fluorescence intensity (Figure 7C). Further, signalling of the ribosensor was maintained up to 7 h after the initial addition of AdoCbl (Figure 7C), indicative of a stable signal, which is not perturbed by external factors or biochemical conversion of B12. Lastly, we confirmed that dose-dependent responses could not be attributed to differential growth of *M. tuberculosis*, since the bacterial growth measured by optical density remained unaltered in the presence of different B12 concentrations (Figure 7C). Nevertheless, this biosensor presents limitations, such as a narrow dynamic range and a limited utility outside of a biosafety laboratory. In addition, a gain in fluorescence signal after incubation with B12 would result in a more desirable outcome than the fluorescence loss reported here. This latter problem could be solved by the use of genetic circuits, but the limited repertoire of genetic tools for the fastidious pathogens of the *Mycobacterium* genus leaves these refinements out of the scope of the present manuscript.

To summarise, we have used genetic, microbiological, and molecular biology evidence to select the most appropriate riboswitch in order to construct a B12 biosensor in *M. tuberculosis*. This ribosensor has demonstrated robust, immediate, and stable sensing of a concentration as low as 0.1 μg/mL of AdoCbl.

3 | Discussion

Our phylogenetic analyses revealed a separation of methionine synthases between tuberculous and NTM. However, the subsequent functional characterisation of MetH isoenzymes demonstrated an equivalent B12 dependency in the orthologs of *M. tuberculosis*, *M. canettii* and *M. smegmatis* under the conditions tested. In contrast, our findings with the MetE isoenzyme resembled the results obtained in the phylogenetic comparative. Our analyses of the *metE* riboswitch suggest that the polymorphisms between *M. tuberculosis* and *M. smegmatis* in this B12 regulatory element are putatively responsible for the differential regulation of MetE expression between tuberculous and NTM. We acknowledge that our assays are designed to detect the B12 dependency of MetE and MetH, but they cannot provide a direct measure of their enzymatic efficacy. A more profound enzymatic characterisation of methionine synthases in the *Mycobacterium* genus would provide knowledge about the phenotype–genotype relationships of species-specific polymorphisms, but this work is out of the scope of the present manuscript. Nevertheless, our findings highlight the importance of validating phylogenetic results using functional studies.

In this context, it could be questioned whether our findings are generalizable to clinical isolates of *M. tuberculosis*. In this regard, it is key to remember the high level of conservation of MetE and MetH enzymes, as well as the regulatory *metE* riboswitch in *M. tuberculosis* sequenced genomes, which otherwise correlate with the clonal context of the *M. tuberculosis* Complex. However, there are interesting exceptions to the rule, the most notable being the partial genetic deletion of the *metH* gene in the *M. tuberculosis* CDC1551 strain (Warner et al. 2007). This strain shows B12 growth defects under laboratory conditions and opens interesting avenues to understand the possible implication of B12 levels from the host in isogenic clinical isolates of *M. tuberculosis*.

The lower B12 sensitivity of the *M. smegmatis* MetE enzyme compared to its ortholog in *M. tuberculosis* could be explained on the basis of the ecological niche of each species. While NTM, including the non-pathogenic *M. smegmatis*, are B12 producers (Minias et al. 2021; Campos-Pardos et al. 2024); the MTBC is abrogated in B12 synthesis and assimilates this vitamin from its obligate mammalian hosts (Campos-Pardos et al. 2024). Thus, the *metE* riboswitch in NTM could have evolved to be less responsive to the endogenous B12 produced by this species. In contrast, the MTBC would have maintained a sensitive B12 riboswitch able to detect the subtle changes in B12 levels existing in the intracellular environment. Our findings also demonstrate a complementary role of MetE and MetH isoenzymes in *M. tuberculosis*, which ensure Met synthesis irrespective of the B12 status of the infected cell. Thus, *M. tuberculosis* would synthesise Met in the absence of B12 using MetE, or in the presence of B12 using MetH. However, in *M. smegmatis*, both isoenzymes are functional independently of the B12 status. This finding raises the intriguing question of the conservation of two opposed mechanisms of Met synthesis in *M. smegmatis*. In this context, it is tempting to speculate that either MetE or MetH are used as the preferred source of Met in this bacterium. Supporting this assumption, examination of RNA-seq profiles in *M. tuberculosis* H37Rv (Solans et al. 2014) and *M. smegmatis* mc^{2}155 (Shell et al. 2015) cultured under standard conditions, shows species-specific expression of methionine synthases. While *M. tuberculosis* expresses high levels of *metE* and *metH* transcripts, *M. smegmatis* exhibits a strong expression of *metE* but a negligible transcription of the *metH* gene (Figure S7). These results would suggest that MetE is the preferred enzyme for Met synthesis in *M. smegmatis* and reconcile our finding that the *M. smegmatis metE* riboswitch is less sensitive to the endogenous B12 produced by these species. The hypothesis that B12 producers harbour more permissive riboswitches to B12 inhibition might also be applied to other *Mycobacterium* species different from *M. smegmatis*. Notably, opportunistic pathogens such as *M. abscessus*, *M. avium* or *M. fortuitum* are also B12 producers (Minias et al. 2021; Campos-Pardos et al. 2024), and they can have evolved permissive riboswitches to B12 inhibition as a compensatory mechanism.

Our previous findings that the MTBC has evolved to depend on host B12 to develop a complete virulence (Campos-Pardos et al. 2024), together with the importance of the B12-dependent synthesis of Met, open interesting perspectives to use the Met metabolism as a druggable target in the MTBC. Indeed, it has been recently shown that MetE is expressed in actively replicating mycobacteria (Iacobino et al. 2024), and also in sputum from TB-infected patients (Hadizadeh Tasbiti et al. 2022) reinforcing its potential use as a drug target. It is tempting to propose the use of B12 analogs able to repress the *metE* riboswitch, and at the same time able to block MetH. However, it is important to remember that B12 is used as a vitamin by mammals, and B12-based drugs should be highly specific against the bacterial targets without affecting the host metabolism.

Lastly, we have applied our knowledge of Met metabolism in the *Mycobacterium* genus in a biotechnological context. We reasoned that the improved sensitivity and selectivity of the *M. tuberculosis metE* riboswitch could be used to construct a whole-cell B12 ribosensor. It is key to remember that the fastidious growth of *M. tuberculosis*, as well as its biosafety requirements, the limited repertoire in genetic tools compared to other bacteria, and the difficulties in incorporating exogenous genetic material, make synthetic biology approaches in this bacterium challenging. Thus, we used a rationale design to identify the *metE* promoter and riboswitch to construct a B12 ribosensor in *M. tuberculosis*. We are aware that further refinement of the genetic parts of the ribosensor could provide enhanced sensitivity, but we encounter the inherent difficulties to achieve this goal in *Mycobacterium*. Nevertheless, this ribosensor strain could open interesting perspectives to understand how the B12 status of a TB-infected host could impact *M. tuberculosis* virulence. On the other hand, ribosensor strains could be used as whole-cell screening platforms to detect B12-based inhibitors of Met metabolism, which could be used as drugs against TB or other bacterial diseases.

4 | Experimental Procedures

4.1 | Bacterial Strains and Growth Conditions

Mycobacteria were cultured at 37°C in Middlebrook 7H9 liquid medium (Difco) supplemented with 10% (v/v) of Middlebrook ADC (0.2% dextrose, 0.5% bovine serum

albumin, 0.085% NaCl and 0.0003% beef catalase) growth supplement and with 0.05% (v/v) Tween 80 (Sigma). For cultures in solid media, Middlebrook 7H10 agar (Difco) was used and supplemented with 10% (v/v) of ADC. In the in vitro growth characterisation assays, both liquid and solid media were supplemented with different isoforms of B12 (AdoCbl, MeCbl, OHCbl and CNCbl) (Sigma) at concentrations ranging from 0.001 to 200 μg/mL. For the construction of mutant strains, 0.2% (w/v) acetamide was used for the induction of the expression of the recombineering proteins Gp60 and Gp61. To select plasmids and mutant strains, 50 μg/mL hygromycin (Hyg) or 20 μg/mL kanamycin (Kan) were added when necessary. *Escherichia coli* DH10B was used in some genetic engineering techniques. This strain was grown in Luria-Bertani (LB) broth or in solid media LB agar at 37°C, or at 30°C for the recombineering event in the case of pKD46 temperature-sensitive plasmid containing strains. When required, medium was supplemented with ampicillin (Amp, 100 μg/mL) or kanamycin (Kan, 20 μg/mL). Arabinose 0.15% was used for induction of recombineering proteins codified in pKD46 plasmid. Manipulation of non-pathogenic mycobacterial strains was performed in a biosafety level 1 (BSL1) and BSL2 laboratories with facilities notifications A/ES/10/I-05 and A/ES/06/I-02, respectively. Manipulation of virulent mycobacterial strains was performed in a BSL3 laboratory with facilities notification A/ES/04/I-05.

4.2 | Phylogenetic Analyses of MetH and MetE in the *Mycobacterium* Genus

Searching for protein sequences was done with PSI-BLAST against the NCBI nr database (Sayers et al. 2022). Proteomes from MTBC (114): *M. canettii* (4), *M. africanum* (26), *M. bovis* (40), *M. tuberculosis* (44) and NTM (39) with query coverage ≥ 75% were analysed (Table S1). Multiple sequence alignments (MSA) were done with Clustal Omega (Sievers and Higgins 2018) (https://www.ebi.ac.uk/jdispatcher/msa/clustalo) and trimmed following the protocol of trimAL (Capella-Gutiérrez et al. 2009). A maximum likelihood phylogenetic tree using the Subtree Pruning and Regrafting (SPR) method was constructed with PhyML (https://ngphylogeny.fr; (Lemoine et al. 2019)). The likelihood aLRT (approximate likelihood-ratio test) statistical test and a bootstrap value of 500 were used. The tree and cladogram were midpoint-rooted and plotted with FigTree (http://tree.bio.ed.ac.uk/software/figtree).

4.3 | Construction of Mutant Strains in *M. tuberculosis*

Deletion of *metH* was achieved using the BAC-recombineering (BAC-rec) strategy (Aguilo et al. 2017). Briefly, the thermosensitive plasmid pKD46 containing the red recombinase from lambda phage (Datsenko 2000) was co-transformed into the *E. coli* DH10B clone carrying BAC Rv73 containing the Rv2124c (*metH*) gene (Brosch et al. 1998). DH10B Rv73 pKD46 transformants incubated with arabinose 0.15% were subsequently transformed with a PCR product obtained using KO BAC Rv2124c FRT Kan-FW (GAGCGC TGTCAACGACTGAGGAAATTTCATAGGCCGACTATC CTTGCCATGTGTAGGCTGGAGCTGCTTC) and KO BAC Rv2124c FRT Kan-RV primers (GCCGACGTCCTGTCG CAGCCGATGCTCCGCACACGTGGGACGGGTCAGACA TATGAATATCCTCCTTAGT). This PCR product consists of a Kan resistance cassette (Kan^R), with FRT sites from pKD4, flanked by 40 bp identity arms to the gene of interest. Recombinants were selected on LB agar containing Kan incubated at 30°C overnight, and gene deletion in the BAC was confirmed by PCR amplification using Conf-KO BAC metH-FW (TTCGGTGGGTGCGACACATAGT) and Conf-KO BAC metH-RV (TCATCGCCCAGGTGTTGGACTG). Allelic exchange substrate (AES) containing the Kan^R flanked by approximately 1 kb identity arms for site-specific recombination was obtained by high fidelity PCR using BAC Rv73-Δ*metH*::Kan^R as a template and Conf-KO Mtb metH-FW (TTCGGCGATCGTCTCGGTGATC) and Conf-KO Mtb metH-RV (TGCGCTATCTGGCTGTTGAGCT) primers. AES was transformed by electroporation into *M. tuberculosis* H37Rv carrying the pJV53H recombineering plasmid (van Kessel and Hatfull 2007) and cultured in the presence of 0.2% acetamide. The *M. tuberculosis* H37Rv Δ*metE*::Kan^R mutant was constructed using a synthetic AES (GenScript) introduced in H37Rv-pJV53H by electroporation. To favour the recombination event and recovery of recombinants, the transformation mixtures were incubated overnight in liquid medium without antibiotic and in the presence of AdoCbl, since MetH requires B12 as a cofactor. For the final steps of mutant construction and confirmation, recombinant colonies were selected by plating on 7H10-ADC with the appropriate antibiotic/supplement and confirmed by PCR using specific primers.

4.4 | Construction of Mutant Strains in *M. smegmatis*

To construct a *metE* knockout in *M. smegmatis* mc^2155 and to mimic the B12 phenotype of *M. tuberculosis*, B12 synthesis in mc^2155 was first abrogated by deletion of the *cobLMK* genes. *M. smegmatis* mc^2155 carrying pJV53H were electroporated with AES containing the Kan^R flanked by approximately 50 bp identity arms for site-specific recombination. The AES was synthesised by PCR amplification of the Kan^R cassette of pKD4 using primers containing 50 bp identity arms KO cobLMK Msmeg FRT Kan-FW (CTGGCGCAGGATGCCGCGATGAGC G C T C A T G C G A A G A G C C G A G G A C A C CGGTGTAGGCTGGAGCTGCTTC) and KO cobLMK Msmeg FRT Kan-RV (GAGCGCCCCGTGGTCAGGAACACG C GCGAAAACCCGCGCTGCGCCACCACCATATGAATAT CCTCCTTAGT). Transformants were plated on 7H10-ADC-Kan plates, and recombinants were confirmed by PCR using specific primers. Once constructed, the *M. smegmatis* mc^2155 Δ*cobLMK*::Kan^R strain, and after confirming pJV53H curation, this strain was electroporated with the pRES-FLP-Mtb plasmid (Song 2007; Pérez et al. 2020) to resolve the Kan^R resistance cassette. The resolved strain was transformed again with the pJV53H to subsequently generate the *metE* mutant. The AES-which contained a Kan^R cassette and the GFP gene optimised for its expression in mycobacteria (eGFP) was synthesised by GenScript. Construction was confirmed by PCR of transformant colonies grown on 7H10-ADC-Kan supplemented with AdoCbl.

4.5 | Bioinformatics Analysis of the *metE* Riboswitch Sequence

The sequence of the *metE* riboswitch in *M. tuberculosis* H37Rv was originally predicted (Vitreschak et al. 2003; Warner et al. 2007), and further refined by exploration of our RNA-seq data (Solans et al. 2014; Campos-Pardos et al. 2024). This sequence was used as a query sequence to identify similar nucleotide sequences in an online BLASTN search against the NCBI Nucleotide database (Sayers et al. 2022). Sequences from the species *M. mungi* (taxid: 1844474) and *M. pinnipedii* (taxid: 194542) were excluded from the subsequent analysis for lack of sequence similarity. The riboswitch sequence for each *Mycobacterium* strain was obtained by comparison with reference genomes annotated in the Mycobrowser database (https://mycobrowser.epfl.ch). After multiple alignments, a tree was obtained with MEGA X (Stecher and Tamura 2020) using the Tamura-Nei model (Tamura 1993), selecting the topology with the highest log likelihood value. The location of the B12 aptamer and stem loop sequences in *M. tuberculosis* was based on the previous secondary structure prediction of the riboswitch (Kipkorir et al. 2024). Stem loops in *M. smegmatis* were predicted using the RNAfold Web server (Gruber et al. 2008). The putative −10 mycobacterial sequence was predicted only using the BPROM algorithm (http://www.softberry.com/berry.phtml?topic=bprom) (Solovyev 2011).

4.6 | Cell Viability Assays

Solutions of AdoCbl (1 mg/mL), MeCbl (1 mg/mL) and CNCbl (1 mg/mL) were all diluted to a concentration of 200 μg/mL. All compounds were serially 10-fold diluted using liquid medium Middlebrook 7H9 supplemented with 0.05% Tween-80 and 10% Middlebrook-ADC (25 μg/mL L-Met when required) in 96-well flat-bottom plates (Nunc Edge 96-Well, Thermo Fisher), with final volumes of 90 μL per well. Stationary-phase bacterial cultures were then diluted to a concentration of 4×10^5 CFU/mL in mycobacteria liquid medium. The diluted bacteria (90 μL per well) were added to the diluted cobalamin isoforms to yield cobalamin concentrations ranging from 0.001 to 100 μg/mL and 2×10^5 CFU/mL bacteria per well. The plate was incubated at 37°C for 48 h. Optical density at 600 nm (OD_{600}) was measured every 15 min with a Synergy HTX plate reader (Biotek) after a previous 10-s linear shaking (567 cpm). To evaluate cell viability after the 48-h incubation, 5 μL from each well were spotted onto 7H10 with 0.05% (v/v) glycerol supplemented with 10% (v/v) ADC and with 25 μg/mL L-Met when needed (Nunc OmniTray Single-Well plates, Thermo Fisher). Plates were incubated for 24 h. Cell metabolic activity after 48 h was assessed with an MTT (3-(4,5-dimethylthiazol-2-yl)- 2,5-diphenyltetrazolium bromide)-based assay. MTT is a redox reporter of metabolic activity and, therefore, bacterial growth. Only metabolically active bacteria are able to reduce MTT (yellow) to the corresponding formazan product (deep purple). After finishing the 48 h incubation at 37°C, 30 μL of a 2.5 mg/mL MTT solution (MTT reagent [Sigma] dissolved in phosphate buffered saline [PBS] and 10% [v/v] Tween-80 [Scharlau]) were added to each well and incubated for 3 h at 37°C. Plates were then analysed with Synergy HTX plate reader (Biotek) for the absorbance at 580 nm. The net absorbance was determined by comparing the absorbance reading of each set of test wells to the control wells containing diluted Cbl isoforms in liquid medium Middlebrook 7H9 supplemented with 0.05% (v/v) Tween 80 and 10% (v/v) Middlebrook-ADC. Readouts were used to determine the MIC_{50} (Minimum Inhibitory Concentration), defined as the minimal concentration of cobalamin isoforms that inhibited MTT conversion by 50% compared to the control.

4.7 | Construction of *M. tuberculosis* Ribosensor Strain

A synthetic sequence containing the promoter and B12-riboswitch of *metE* from *M. tuberculosis* H37Rv fused to the *eGFP* gene was synthesised by Genescript and cloned into the pMV361H integrative plasmid, which confers Hyg resistance. This plasmid was named pMV361H- Pr+RbSw(metE)_eGFP, or 'ribosensor' plasmid, for clarity. Electrocompetent cells of *M. tuberculosis* H37Rv were transformed with the pMV361H- Pr+RbSw(metE)_eGFP plasmid. The transformants were selected on 7H10-OADC-Hyg plates, and the integration of the plasmid in the transformants was analysed by PCR. Liquid cultures derived from the PCR-positive colonies were grown and reanalysed by PCR to confirm maintenance of the transformed plasmid.

4.8 | Fluorescence Measurements

Bacterial cultures of the ribosensor strain were diluted to a concentration of 4×10^5 CFU/mL in 7H9-ADC medium. The diluted bacteria (90 μL per well) were added to the diluted Cbl isoforms to yield Cbl concentrations of 0.01, 0.1, 1, 10 and 100 μg/mL, along with 2×10^5 CFU/mL bacteria per well. The plate was incubated at 37°C for the desired times. OD_{600} and bottom fluorescence (485 nm excitation, 525 nm emission) were measured with a SpectraMax iD3 Multi-Mode Microplate Reader (Molecular Devices).

4.9 | Statistical Analysis

Data are presented as individual data points, with bars indicating the mean. In some cases, error bars representing the standard deviation (SD) or the standard error of the mean (SEM) were included. Statistical analyses were conducted using GraphPad Prism 8.0. For multiple group comparisons, one-way ANOVA followed by Dunnett's test corrected for multiple comparisons was performed. P values < 0.05 were considered significant. The number of stars means $*p < 0.05$; $**p < 0.01$; $***p < 0.001$ and $****p < 0.0001$.

Author Contributions

Elena Campos-Pardos: conceptualization, investigation, methodology, validation, visualization, formal analysis. **Laura Sanz-Asensio:** conceptualization, investigation, writing – original draft, methodology, validation, visualization, writing – review and editing, formal analysis. **Sandra Pérez-Jiménez:** conceptualization, investigation, methodology, validation, visualization, software, formal analysis. **Inmaculada Yruela:** investigation, methodology, software. **Bruno Contreras-Moreira:** investigation, methodology, software. **Alejandro Toledo-Arana:** writing – review and editing, formal analysis, investigation,

conceptualization, validation. **Jesús Gonzalo-Asensio:** conceptualization, investigation, funding acquisition, writing – original draft, methodology, validation, visualization, writing – review and editing, project administration, supervision.

Acknowledgements

The authors would like to acknowledge the use of the BSL3 facilities from 'Servicio General de Apoyo a la Investigación-SAI' of the University of Zaragoza. This work was supported by grants PID2019-104690RB-I00 and PID2023-148710OB-I00 funded by MCIN/AEI/10.13039/501100011033 to Jesús Gonzalo-Asensio, a grant FPU17/02909 funded by the Spanish Ministry of Universities to Elena Campos-Pardos, and a grant funded by Gobierno de Aragón during the period 2023-2027 to LSA.

Conflicts of Interest

The authors declare no conflicts of interest.

Data Availability Statement

The biological material described in the manuscript will be accessible upon request to the corresponding author.

References

Aguilo, N., J. Gonzalo-Asensio, S. Alvarez-Arguedas, et al. 2017. "Reactogenicity to Major Tuberculosis Antigens Absent in BCG Is Linked to Improved Protection Against *Mycobacterium tuberculosis*." *Nature Communications* 8: 16085.

Brosch, R., S. V. Gordon, A. Billault, et al. 1998. "Use of a *Mycobacterium tuberculosis* H37Rv Bacterial Artificial Chromosome Library for Genome Mapping, Sequencing, and Comparative Genomics." *Infection and Immunity* 66: 2221–2229.

Broset, E., C. Martín, and J. Gonzalo-Asensio. 2015. "Evolutionary Landscape of the *mycobacterium tuberculosis* Complex From the Viewpoint of phoPR: Implications for Virulence Regulation and Application to Vaccine Development." *MBio* 6: e01289.

Campos-Pardos, E., S. Uranga, A. Picó, A. B. Gómez, and J. Gonzalo-Asensio. 2024. "Dependency on Host Vitamin B12 has Shaped *Mycobacterium tuberculosis* Complex Evolution." *Nature Communications* 15: 1–13.

Capella-Gutiérrez, S., J. M. Silla-Martínez, and T. Gabaldón. 2009. "trimAl: A Tool for Automated Alignment Trimming in Large-Scale Phylogenetic Analyses." *Bioinformatics* 25: 1972–1973.

Cole, S., R. Brosch, J. Parkhill, et al. 1998. "Deciphering the Biology of *Mycobacterium tuberculosis* From the Complete Genome Sequence." *Nature* 393: 537–544.

Cortes, T., O. T. Schubert, G. Rose, K. B. Arnvig, I. Comas, and R. Y. D. Aebersold. 2013. "Genome-Wide Mapping of Transcriptional Start Sites Defines an Extensive Leaderless Transcriptome in *Mycobacterium tuberculosis*." *Cell Reports* 5: 1121–1131.

Datsenko, K. A. 2000. "One-Step Inactivation of Chromosomal Genes in *Escherichia coli* K-12 Using PCR Products." *Proceedings of the National Academy of Sciences of the United States of America* 97: 6640–6645.

Gopinath, K., A. Moosa, and V. Mizrahi. 2013. "Vitamin B12 Metabolism in *Mycobacterium tuberculosis*." *Future Microbiology* 8: 1405–1418.

Goulding, C. W., D. Postigo, and R. G. Matthews. 1997. "Cobalamin-Dependent Methionine Synthase Is a Modular Protein With Distinct Regions for Binding Homocysteine, Methyltetrahydrofolate, Cobalamin, and Adenosylmethionine." *Biochemistry* 36: 8082–8091.

Gruber, A. R., R. Lorenz, S. H. Bernhart, R. Neuböck, and I. L. Hofacker. 2008. "The Vienna RNA Websuite." *Nucleic Acids Research* 36: 70–74.

Hadizadeh Tasbiti, A., F. Badmasti, S. D. Siadat, A. Fateh, F. Yari, and M. GHzanfari Jajin. 2022. "Recognition of Specific Immunogenic Antigens With Potential Diagnostic Value in Multi-Drug Resistant *Mycobacterium tuberculosis* Inducing Humoral Immunity in MDR-TB Patients." *Infection, Genetics and Evolution* 103: 105328.

Hodgkin, D., J. Pickworth, J. Robertson, D. C. Hodgkin, and J. H. Robertson. 1955. "Structure of Vitamin B12: The Crystal Structure of the Hexacarboxylic Acid Derived From B12 and the Molecular Structure of the Vitamin." *Nature* 176: 325–328.

Iacobino, A., R. Teloni, C. Mancone, et al. 2024. "Identification of Rv1133c (MetE) as a Marker of *Mycobacterium tuberculosis* Replication and as a Highly Immunogenic Antigen With Potential Immunodiagnostic Power." *Frontiers in Immunology* 15: 1464923.

Jang, J., J. Becq, B. Gicquel, and P. N. O. Deschavanne. 2008. "Horizontally Acquired Genomic Islands in the Tubercle Bacilli." *Trends in Microbiology* 16: 303–308.

Jarrett, J. T., M. Amaratunga, C. L. Drennan, et al. 1996. "Mutations in the B12-Binding Region of Methionine Synthase: How the Protein Controls Methylcobalamin Reactivity." *Biochemistry* 35: 2464–2475.

Kipkorir, T., P. Polgar, D. Barker, A. D'Halluin, and Z. A. K. Patel. 2024. "A Novel Regulatory Interplay Between Atypical B 12 Riboswitches and uORF Translation in *Mycobacterium tuberculosis*." *Nucleic Acids Research* 52: 7876–7892.

Lemoine, F., D. Correia, V. Lefort, et al. 2019. "NGPhylogeny.Fr: New Generation Phylogenetic Services for Non-Specialists." *Nucleic Acids Research* 47: W260–W265.

Minias, A., F. Gąsior, A. Brzostek, T. Jagielski, and J. Dziadek. 2021. "Cobalamin Is Present in Cells of Non-Tuberculous Mycobacteria, but Not in *Mycobacterium tuberculosis*." *Scientific Reports* 11: 12267.

Nahvi, A., J. E. Barrick, and R. R. Breaker. 2004. "Coenzyme B12 Riboswitches Are Widespread Genetic Control Elements in Prokaryotes." *Nucleic Acids Research* 32: 143–150.

Pejchal, R., and M. L. Ludwig. 2005. "Cobalamin-Independent Methionine Synthase (MetE): A Face-to-Face Double Barrel That Evolved by Gene Duplication." *PLoS Biology* 3: 254–265.

Pérez, I., S. Uranga, F. Sayes, et al. 2020. "Live Attenuated TB Vaccines Representing the Three Modern *Mycobacterium tuberculosis* Lineages Reveal That the Euro-American Genetic Background Confers Optimal Vaccine Potential." *eBioMedicine* 55: 102761.

Riojas, M. A., K. J. McGough, C. J. Rider-Riojas, N. Rastogi, and M. H. Hazbón. 2018. "Phylogenomic Analysis of the Species of the *Mycobacterium tuberculosis* Complex Demonstrates That *Mycobacterium africanum*, *Mycobacterium bovis*, *Mycobacterium caprae*, Mycobacterium Microti and *Mycobacterium pinnipedii* Are Later Heterotypic Synonyms of Mycob." *International Journal of Systematic and Evolutionary Microbiology* 68: 324–332.

Roth, J. R., J. G. Lawrence, and T. A. Bobik. 1996. "Cobalamin: Synthesis and Biological Significance." *Annual Review of Microbiology* 50: 137–181.

Sayers, E. W., E. E. Bolton, J. R. Brister, et al. 2022. "Database Resources of the National Center for Biotechnology Information." *Nucleic Acids Research* 50: D20–D26.

Shell, S. S., J. Wang, P. Lapierre, et al. 2015. "Leaderless Transcripts and Small Proteins Are Common Features of the Mycobacterial Translational Landscape." *PLoS Genetics* 11: e1005641.

Shelton, A. N., E. C. Seth, K. C. Mok, et al. 2019. "Uneven Distribution of Cobamide Biosynthesis and Dependence in Bacteria Predicted by Comparative Genomics." *ISME Journal* 13: 789–804.

Sievers, F., and D. G. Higgins. 2018. "Clustal Omega for Making Accurate Alignments of Many Protein Sequences." *Protein Science* 27: 135–145.

Snapper, S., R. Melton, S. Mustafa, T. Kieser, and W. J. Jacobs. 1990. "Isolation and Characterization of Efficient Plasmid Transformation Mutants of *Mycobacterium smegmatis*." *Molecular Microbiology* 4: 1911–1919.

Solans, L., J. Gonzalo-Asensio, C. Sala, et al. 2014. "The PhoP-Dependent ncRNA Mcr7 Modulates the TAT Secretion System in *Mycobacterium tuberculosis*." *PLoS Pathogens* 10: e1004183.

Solovyev, V. 2011. "Automatic Annotation of Microbial Genomes and Metagenomic Sequences." Metagenomics Its Applications Agriculture Biomedicine Environmental Studies. 61–78.

Song, H. 2007. "Functional Expression of the Flp Recombinase in *Mycobacterium bovis* BCG." *Gene* 399: 112–119.

Stecher, G., and K. Tamura. 2020. "Molecular Evolutionary Genetics Analysis (MEGA) for macOS." *Molecular Biology and Evolution* 37: 1237–1239.

Supply, P., M. Marceau, S. Mangenot, et al. 2013. "Genomic Analysis of Smooth Tubercle Bacilli Provides Insights Into Ancestry and Pathoadaptation of *Mycobacterium tuberculosis*." *Nature Genetics* 45: 172–179.

Tamura, K. 1993. "Estimation of the Number of Nucleotide Substitutions in the Control Region of Mitochondrial DNA in Humans and Chimpanzees." *Molecular Biology and Evolution* 10: 512–526.

van Kessel, J., and G. Hatfull. 2007. "Recombineering in *Mycobacterium tuberculosis*." *Nature Methods* 4: 147–152.

Vitreschak, A. G., D. A. Rodionov, A. A. Mironov, and M. S. Gelfand. 2003. "Regulation of the Vitamin B12 Metabolism and Transport in Bacteria by a Conserved RNA Structural Element." *RNA* 9: 1084–1097.

Warner, D. F., S. Savvi, V. Mizrahi, and S. S. Dawes. 2007. "A Riboswitch Regulates Expression of the Coenzyme B12- Independent Methionine Synthase in *Mycobacterium tuberculosis*: Implications for Differential Methionine Synthase Function in Strains H37Rv and CDC1551." *Journal of Bacteriology* 189: 3655–3659.

Warren, M. J., E. Raux, H. L. Schubert, and J. C. Escalante-Semerena. 2002. "The Biosynthesis of Adenosylcobalamin (Vitamin B12)." *Natural Product Reports* 19: 390–412.

World Health Organization. 2024. "Global Tuberculosis Report 2024."

Young, D. B., I. Comas, and L. P. S. de Carvalho. 2015. "Phylogenetic Analysis of Vitamin B12-Related Metabolism in *Mycobacterium tuberculosis*." *Frontiers in Molecular Biosciences* 2: 1–14.

Supporting Information

Additional supporting information can be found online in the Supporting Information section.